

COST BENEFIT ANALYSIS FOR ROCK-SIDE SLOPE FAILURE PREVENTION USING RELIABILITY BASED DESIGN

H. M. ADEL¹, S. A. AKL² AND Y. A. HEGAZY³

ABSTRACT

This paper examines the financial benefits of rockslide prevention measures at Gebel Mokattam area, where the catastrophic rock failure accident that occurred in (06/09/2008) in Duwaiqa area, Cairo, Egypt. A frequency ratio index (FRI) was achieved based on the rockslide-related geological and climate factors (e.g. slope, aspect, curvature, and precipitation), which highlights the main rockslide conditioning features and the most hazardous and weak sectors in Mokattam area. FRI represents the ratio of the rockslide occurrence probabilities to the non-occurrence probabilities for a given class within a factor. Results showed that slope was the most hazardous factor controlling the rock failure in Mokattam. The rock-side slope was supported by using rock bolts to improve slope stability and consequently preventing the rockslide accidents. Findings will guide geotechnical engineers to choose optimal R.I which meets optimal and effective total costs. The most critical parameters; uniaxial compressive strength (UCS) and geological strength index (GSI) were applied and evaluated in this study, in addition to analyzing their different nine scenarios to reach the optimal total cost of the slope stability which meets the optimal reliability index.

KEY WORDS: Rock failure, Reliability, Slope stability, Frequency ratio index, Cost optimization.

1. INTRODUCTION

The characterization of rock masses for engineering applications is subject to uncertainties due to the limited data that are typically available during site characterization, and due to inherent variability of properties within the rock mass. As known that the uncertainty in geological system stems [1] from variability caused by random process (Aleatory), which is: a) Natural variability in rock mass; b) Natural

¹ Ph. D. Candidate, Soil Mechanics and Foundations, Public Works Department, Faculty of Engineering, Cairo University, Giza, Egypt, haithamsorour@hotmail.com

² Associate Professor, Soil Mechanics and Foundations, Public Works Department, Faculty of Engineering, Cairo University, Giza, Egypt.

³ Professor, Soil Mechanics and Foundations, Public Works Department, Faculty of Engineering, Cairo University, Giza, Egypt.

variability in in-situ stress parameters; and c) Knowledge-based uncertainty that exists due to lack of information (Epistemic), which includes: a) Site characterization uncertainty b) Parameter uncertainty c) Model uncertainty [2]. Reliability-based design will be used as an approach to incorporate possible uncertainties values in the design. However, the results are affected by the assumed distribution and statistical parameters of the rock properties. Within that context, hazard assessment and the quantification of the probability of undesirable events, i.e., failure probability is a significant aspect of the decision-making process. In general, most computer software require Mohr-Coulomb soil parameters (C' and ϕ') as input, thus ignoring the non-linear nature of the rock mass failure envelope. Furthermore, the non-linearity is more pronounced at the low confining stresses that are operational in slope stability problems [3]. As discussed by [4], the Hoek-Brown failure criterion is one of the few non-linear criteria used by practicing engineers to estimate rock mass strength. Latest version of Hoek–Brown yield criterion is expressed by Eqs. (1-4).

$$\sigma_1' = \sigma_3' + \sigma_{ci} ((mb \sigma_3' / \sigma_{ci}) + (s))^\alpha \quad (1)$$

$$mb = m_i \exp ((GSI-100) / (28-14D)) \quad (2)$$

$$s = \exp ((GSI-100) / (9-3D)) \quad (3)$$

$$\alpha = (1/2) + ((1/6)(e^{-GSI/15} - e^{-20/3})) \quad (4)$$

With the magnitudes of mb , s and α rely on the geological strength index (GSI), which describes the rock mass quality, and σ_{ci} and m_i representing the intact uniaxial compressive strength (UCS) and material constant respectively. The parameter D is a factor that depends on degree of disturbance which ranges between zero and one. Currently, Li et al. [5] provided both the numerical upper and lower bound solutions for rock slope assessments based on the Hoek Brown failure criterion. In [5], a new non dimensional stability number (N) was proposed. It is based on the Hoek Brown failure criterion and defined by Eq. (5).

$$N = \sigma_{ci} / \gamma HF \quad (5)$$

Where γ is unit weight of the rock mass, and H and F are the height and the safety factor of the slope respectively. The safety factor [5] was presented in terms of $\sigma_c / \gamma H$ as these three parameters can be directly measured more easily and accurately, compared with other strength parameters of the Hoek–Brown yield criterion. However, the definition in safety factor for Eq. 5 is different from that of conventional factor of safety used in limit equilibrium analysis [6], as shown in Eq. (6).

$$F_s = \Sigma (\text{resisting actions}) / \Sigma (\text{driving actions}) \quad (6)$$

Although both safety factors F and F_s represent a failure when they equal one, due to their different definition they generally are not equal (i.e. $F \neq F_s$) [7].

Rockslides are one of the most historical natural hazards along with earthquakes and floods. For this reason, hazard and risk assessment has been the main aim of numerous scientific papers, focusing on geomorphological and multidisciplinary or statistical approaches [8]. The level of risk is mostly defined as the intersection of hazard with the value of the elements at risk by way of their susceptibility. This assumption is usually based on a great number of variables; susceptibility of element at risk is closely related to the kind of rockslide, and frequency based hazard assessment often relies on a few periods of knowledge of slope instabilities. Fortunately, previous years' measurements have been thoroughly collected using GIS databases, web information sharing and a greater awareness of rockslide risk [9]. This approach permitted some authors to compute the costs of destructions because of rock slope instabilities within several environments around the world: from 1972 to 2007, landslides and rock failures cost five hundred twenty million EUR and caused 32 victims in Switzerland [10], while in the United States one to two billion USD expense in financial losses and about 25 to 50 deaths per year have been estimated, e.g., nine million USD expense in only direct cost losses in Colorado during 2010 [11]. Historical research indicates that more than 50593 people died, went missing or were injured in 2580 rockslides and floods in Italy, where 26.3 % of the 8102 municipalities have been hit by rock slope instabilities between 1979 and 2002 [12]. In Southern India, the triggering of many rockslides hanging over 20 km long roads could cost from \$ 90840 to \$ 779500, with an average annual total loss estimated at \$ 35000 [13].

These expenses highlight how much people need protective measures against rockslides, which cause billions USD every year in failures and financial losses. Risk management includes the full range of procedures and tasks that ultimately lead to the implementation of rational policies and appropriate measures for risk reduction [14]. The literature offers a variety of different methods to assess risk and financial losses due to rockslide accidents; both of these features represent the central topic when decision makers are called to act toward prevention, and thus an in depth analysis is needed analysis. These maps are next overlaid with information concerning elements at risk and their financial value, defined by maps of probability of direct monetary loss per year or by quantification of financial losses at municipal level [15]. However, other authors focus on a slope scale approach, including this study, in which information on rockslide accidents and local geological and climate features need to be wisely considered. Despite the fact that every accident has to be evaluated one by one, this analysis usually allows quantitative assessment of rockslide costs and losses [16]. Thus, given a specified rockslide accident which caused various damages, costs of rebuilding are well known, while costs related to a potential prevention plan depend on what type of preventive work is chosen and on what business company is selected. Each of the latter features has to be generally evaluated on a case by case basis. In this work, we have considered the effects of an exceptional rock failure accident that happened (06/09/2008) in Duwaiqa area at Gebel Mokattam, Cairo, Egypt, to perform a cost/benefit analysis of rockslide prevention vs. post event actions. To achieve these goals, the geological and climate rockslide-related factors were delineated in detail using high resolution remote sensing and precipitation datasets (e.g., Digital elevation model (DEM) and Google Earth) and implemented within ArcGIS 10.6 software [17]. Frequency ratio index (FRI) [18] was modeled based on the risk rating of the GIS-based rockslide factors to identify the most affected sectors in Mokattam area to verify potential rock failure occurrence in the future.

2. METHODOLOGY

A model was created for upper plateau in Gebel Mokattam area using RocData and Slide software to find out how safe rock slope stability should be. The methodology flow chart is summarizing the model steps applied in this paper as shown in Fig. 1. The model of the upper plateau estimated from the geology, consists of a single layer of rock and is extended 50 m in the direction of X, 10 m upward from the right side and 5 m upward from the left side in the direction of Y with an angle of inclination 90 degrees as shown in Fig. 2. According to the topography of the selected zone and from the site investigation, it was found that the height of the rocks ranges from 3:00 m to 7:00 m, thus for building the model, a value of 5 m height is taken as an average.

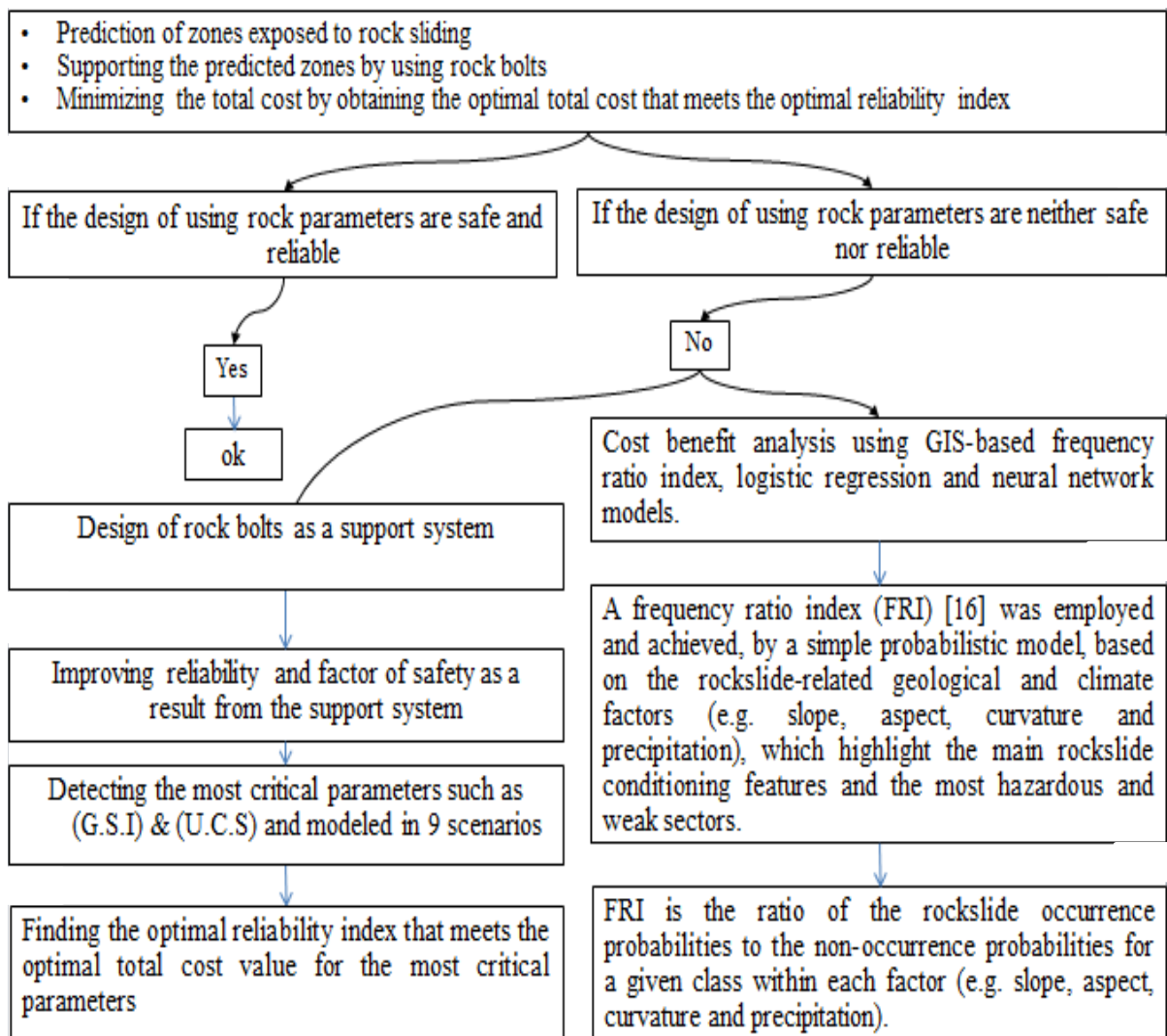


Fig. 1. Methodology flow chart.

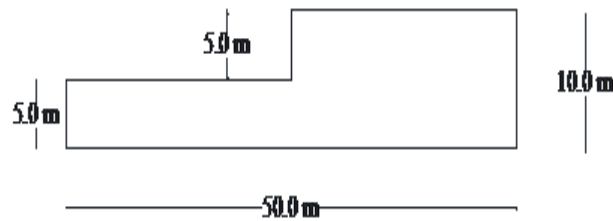


Fig. 2. The proposed model for upper plateau.

FRI is built based on the risk rating of the geological and climate rockslide-related factors (e.g., slope, aspect, curvature and precipitation) that were delineated in detail using high resolution remote sensing and precipitation datasets (e.g., DEM from the Japanese ALOS PALSAR and Google Earth) and implemented within ArcGIS 10.6 software [17], Fig. 3.

The fitted curves were created using data curve fitting (by LABFit software) based on the calculations of construction cost, total failure cost multiplied by (P_f) and total cost. Where the construction cost is equal to length of support multiplied by longitudinal price. While the total failure cost is equal to the sum of the direct and indirect failure costs. The total expected cost is the sum of construction cost and [total failure cost multiplied by (P_f)].

2.1 Study Area

Gebel Mokattam, is located to the east of Cairo, Fig. 3, and has two plateaus that are structurally separated and controlled by major normal faults, Fig. 3a and b. The upper plateau has a steep slope overlooking the eastern side of Cairo with an elevation close to 400 m above sea level, where the catastrophic rockslide failure accident (6/9/2008) in Duwaiqa area Fig. 3d, while the middle plateau has less elevation Fig. 3c. The dominant lithological rocks in Gebel Mokattam area are white, dolomitic fractured limestone beds of middle-late Eocene age, in addition to the clastic sediments; sandstones, and shale, Fig. 3b [19].

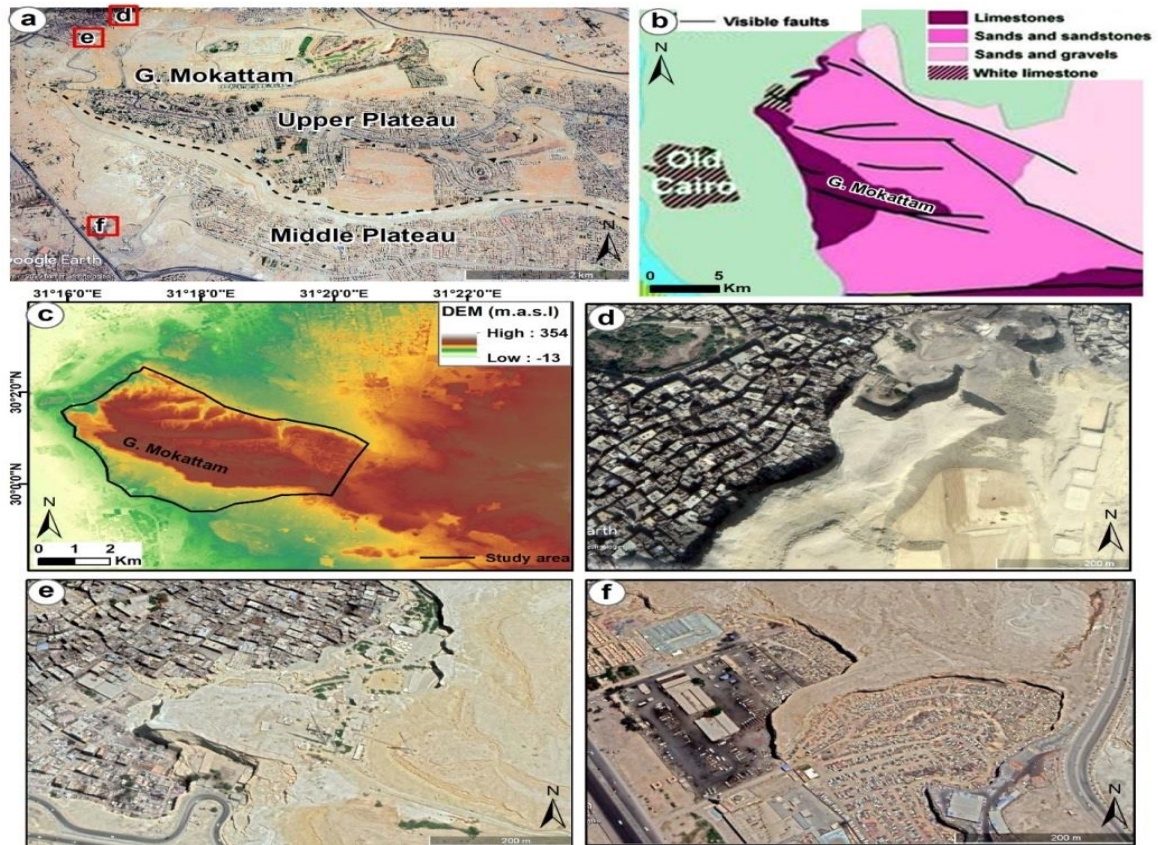


Fig. 3. a) Google Earth image for Mokattam area. b) Geological map modified after [19].
 c) Digital elevation model from ALOS satellite data using ArcGIS 10.6 [17].
 d) Google Earth image for Duwaiqa area e) Google Earth image for upper plateau
 f) Google Earth image for middle plateau.

2.2 Collection and Data Arrangement

Values of the rock parameters were collected and arranged [20]. Subsequently, statistical analysis was calculated for the upper plateau. These values are inserted as input data into RocData software, to get the Hoek-Brown parameters (m & s).

2.3 Calculation of Reliability Index (RI) and Factor of Safety (FS)

To estimate Hoek Brown parameters (m & s), maximum value of each parameter had to be inserted separately with mean values of remaining parameters in RocData software. Previous step repeated, taking into consideration insertion of mean value of each parameter separately with mean values of remaining parameters. Reiteration of previous step had been done through inserting minimum value for each parameter separately, with mean values of the remaining parameters. Afterwards, Hoek-Brown parameters (m & s), for each case, were obtained from RocData

software. Later the Hoek-Brown parameters (m & s), unit weight and (U.C.S) values were entered into Slide software, taking into consideration the suitable statistical distribution for these parameters which thoroughly considered by using LABFit software using Monte Carlo Simulation as shown in Table 1. As a result from the previous steps, the (RI), (FS), and (Pf) for each case were gotten. Table 2 shows RI and FS for the Upper Plateau.

Table 1. Best distribution for upper plateau using LABFit software.

Parameters	Hoek-Brown m parameter	UCS	Unit Weight	Hoek-Brown s parameter
Distribution	Normal	Lognormal	Gamma	Lognormal

It is noted that if the (RI) is ≥ 3 , there is no need for reinforcement (rock bolts) [21]. Otherwise, (RI) must be improved by using rock bolts. Knowing that, RI of at least 3 is recommended as a minimal assurance of a safe slope design [5].

Table 2. Values of RI and FS for the upper plateau in Mokattam area.

Parameters	Material Properties	RI	FS	Material Properties	RI	FS
U.C.S	Max	5.49	2.47	Mean	2.91	1.58
	Min	0.00	1			
G.S.I	Max	4.03	2.23			
	Min	1.23	1.2			
Unit weight	Max	2.74	1.52			
	Min	2.99	1.62			
M _i	Max	3.31	1.62			
	Min	2.53	1.55			
E _i	Max	2.91	1.58			
	Min	2.91	1.58			
D	Max	1.92	1.38			
	Min	3.7	1.87			
Slope Height	Max	2.29	1.39			
	Min	3.35	1.95			

2.4 Length of Rock Bolt and Tensile Strength

To indicate the calculation of the length for rock bolt and tensile strength, for RI lower than the value of 3 we considered the following:

- a) Equivalent cohesion and internal friction (c & φ) from RocData software obtained.
- b) The calculation of the length for rock bolt and tensile strength, using design of rock nail walls of Federal Highway Administration (FHWA) [22], had been applied.

The FHWA presents information on analysis, design, and construction of soil nail walls in highway applications that provide practitioners in this field with sound and simple methods and guidelines that will allow them to analyze, design, and construct safe and economical structures. New probability parameters such as (inclination angle, support length, distance between supports, out of plan spacing, tensile capacity, plate capacity and bond strength) added as input data in Slide software as shown in Table 3.

Table 3. Probability for the rock nails of the upper plateau in Mokattam area.

Parameters	Inclination Angle, °	Support Length, m	Distance Between Supports (S _V), m	Out of Plan Spacing (S _H), m	Tensile Capacity, kN	Plate Capacity, kN	Bond Strength, kN/m
Max	20.00	7.85	2.00	2.12	62.34	751.00	600.00
Mean	15.00	6.63	1.50	1.41	52.82	339.50	500.00
St.dev	3.32	0.39	0.40	0.47	4.79	185.79	79.06
Min	10.00	5.93	1.00	0.71	45.98	118.00	400.00

2.4.1 Determination of total number of supports for upper plateau

There are 3 cases for number of supports in Y direction/ m' according to the value of length of out of plan spacing: a) the 1st case if the out of plan spacing = Max (2.12m), the number of supports will be 1, Fig. 4a; b) the 2nd case if the out of plan spacing = mean (1.41m), the number of supports in will be 2 Fig. 4b; c) the 3rd case if the out of plan spacing = Min (0.71 m), the number of supports will be 3, Fig. 4c.

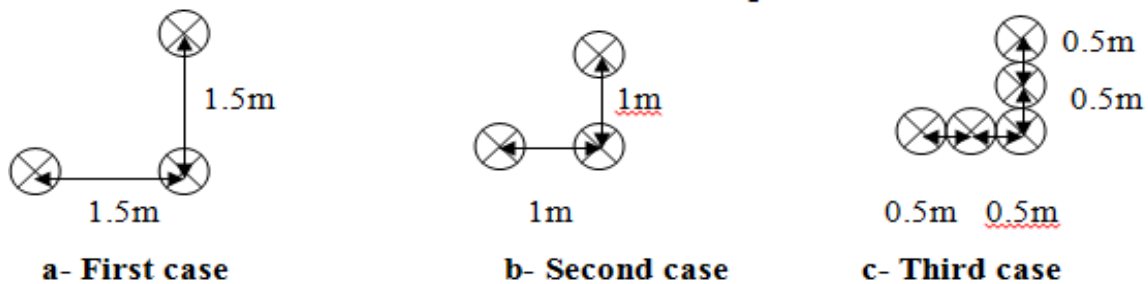


Fig. 4. Different cases of rock nailing support in Y/ m' direction for upper plateau.

There are 3 cases for determination of the number of supports in Z direction according to the value for the distance between supports knowing that this distance between supports ranges (1-2m): a) the 1st case if the distance between supports = maximum (2m), the number of supports in Z direction will be 3; b) the second case if the distance between supports = mean (1.5m), the number of supports in Z direction will be 4; c) the third case if the distance between supports = minimum (1m), the number of supports in Z direction will be 6 as shown in Fig. 5.

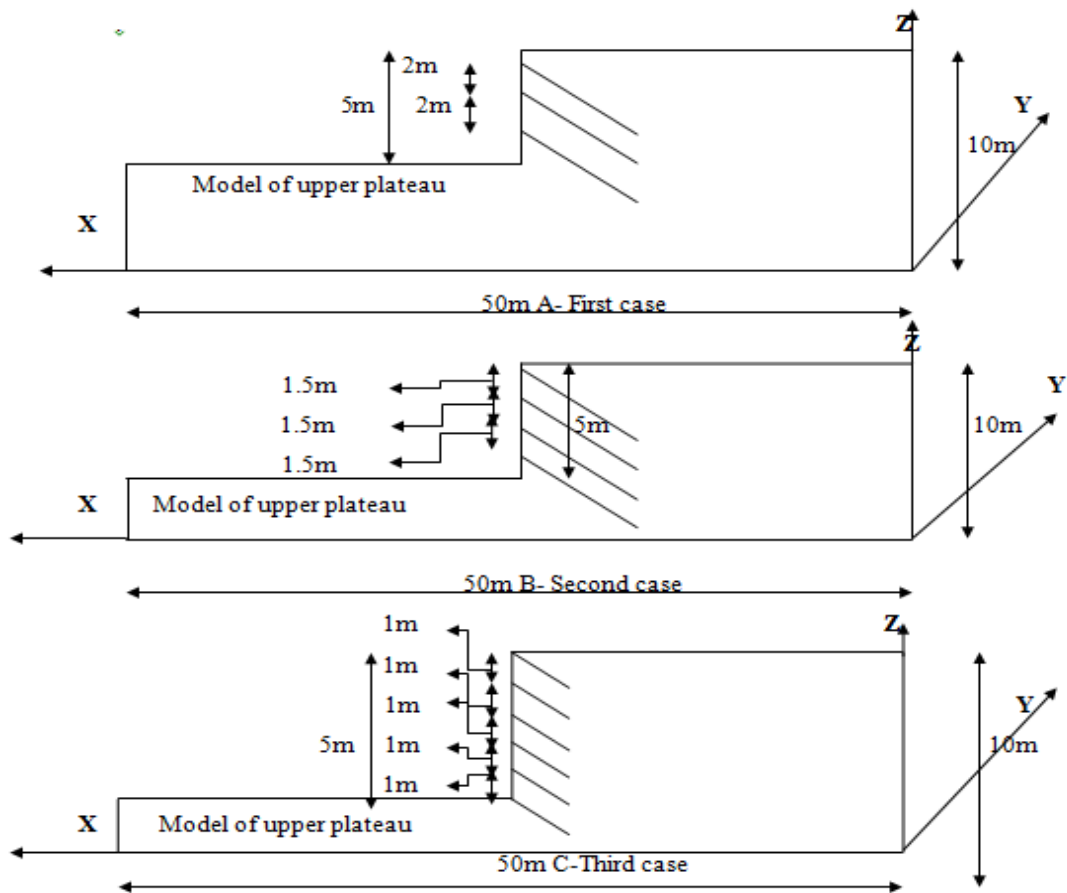


Fig. 5. Different cases of rock nailing support in Z direction for upper plateau.

Eq. (7) should be calculated for each case:

$$N_T = N_Z * N_Y \quad (7)$$

Where N_T is the total number of supports, N_Z is the number of supports in Z direction and N_Y is the number of supports in Y direction/ m' (according to the case studied).

2.5 Identifying the Most Critical Parameters

The values of Hoek-Brown parameters (m&s) were obtained from RocData software for the values of [(Mean + Standard Deviation [SD]), (Mean) and (Mean - SD)] for rock parameters which shown in Table 4. According to the Central Limit Theorem [23] which states that "the sampling distribution of the sample means approaches a normal distribution as the sample size gets larger. This fact holds especially true for sample sizes over 30. In this paper all the studied parameters such as (UCS, Unit Weight and Hoek-Brown's parameters) with samples sizes greater than 30, therefore it was normally distributed with minimum effect on the results.

Table 4. Rock parameters for the upper plateau in Mokattam area.

Parameters	U.C.S, MPa	G.S.I	Unit weight, kN/m ³	Mi	Ei, MPa	D	Slope Height, m
Mean + SD	29.28	42.05	21.79	10.58	6112.44	0.98	6.58
Mean	21.68	37.00	20.94	9.00	4325.36	0.85	5.00
SD	7.60	5.05	0.85	1.58	1787.08	0.13	1.58
Mean - SD	14.09	31.95	20.09	7.42	2538.28	0.72	3.42

Afterwards the [{Hoek- Brown parameters (m&s)}, {Unit weight (kN/m³)} and (U.C.S) (MPa)], values were entered into Slide software (limit equilibrium slope stability analysis), to obtain the RI for each probability of [(Mean + SD), (Mean) and (Mean - SD)]. Considering the suitable statistical distribution for the previous parameters using LABFit software, this was entered as input data in Slide software. In order to calculate the most critical parameter, Eq. (8) is used for each parameter,

$$M_{CP} = R.I \text{ of } (M_+) - R.I \text{ of } (M_-) / 3 \tag{8}$$

Where M_{CP} is the most critical parameter, (M_+) is the (Mean + SD) and (M_-) is the (Mean - SD).

3. COST OPTIMIZATION

There are two reasons why a probability model should supplement the conventional design approach. The 1st reason is to develop a methodology that can handle the limitations of the conventional safety factor method of analysis. The 2nd

reason, and the most important, is to have an expression for side slope failure probability that can be combined with the costs associated with the structure to optimize design. Once the safety of structure is expressed in terms of its $[P_f]$, a design optimization procedure can be developed. This procedure gives the geo-technical engineer a method of determining what $[P_f]$ to design for. In the conventional approach, design safety factors are set based on intuitive judgment and past experience. In many cases, the consequences of failure are overlooked. By combining the consequences of failure with the $[P_f]$ and the construction costs, a logical decision can be made as to the required safety of a structure. Consider a case of rock slope stability by evaluating the $[P_f]$ for different geo-metrical features and by estimating the construction costs for each design. The recommended design $[P_f]$ is that which minimizes the total expected cost (TEC). The above procedure assumed that the consequences of failure are only of a financial nature. This means that the risks of death or badly injury and the major environmental consequences should also be assigned costs. By proceeding with a design optimization approach based on financial considerations, a logical decision can be made as to how safe rock slope stability should be. The probability model assumes that all rock side slopes stability have a calculable (P_f). By recognizing and evaluating this probability, the geo-technical engineer is able to treat it in a logical manner.

3.1 Cost Optimization Calculations of Nine Scenarios

To obtain the equations of the expected total cost, cost of construction and total cost of failure, nine scenarios were estimated using the probability values of the two most critical parameters, (UCS & GSI), that change according to the combinations between the (Mean and SD).

All of the above-mentioned scenarios were calculated to find the values of RI through Slide software, and this is for all the different values that change between Min, Max and Mean, and for (support length, distance between supports and out of plan spacing). Then it is possible to calculate the total length of support as a multiplication of (support length by total number of supports) where the total number of supports is

the summation of number of supports in Y direction/m' plus number of supports in Z direction (as mentioned before in Eq. (7)). After that sorting of the total length of supports and the corresponding RI values in ascending order can be done. These values are converted to the values ranges between zero and one by using the normality index Eq. (9);

$$\frac{(X_{max}-X_i)}{(X_{max}-X_{min})} \quad (9)$$

Where X_{min} is the minimum value of the RI, X_{max} is the maximum value of the RI, and $X_i = 1, 2 \dots \dots i$, (i equal the maximum value of RI).

The previous steps were taken in order to obtain the probability of failure (P_f). Noting that the P_f is equal to (1-R.I).The cost of construction which equals to multiplication of (the total length of support by cost of supports per meter run) was estimated. Then it is possible to estimate the values of direct and indirect cost of failures. The direct cost of failure which equals to the sum of [compensation of loses (properties, lives and injuries), cost of road damages, cost of road recovery and cost of car damages] was evaluated. The indirect cost of failure which equals to the sum of (lawsuits, penalties and reputation) was calculated. This is followed by estimating the total cost of failure which equals to (the sum of direct and indirect cost of failures) multiplied by P_f . These steps lead to evaluate the total expected cost which equals to the sum of construction cost and (total cost of failure multiplied by P_f). The final step includes plotting these values in graphs, where the Y axis represents cost and the X axis represents P_f , to obtain a group of curves includes (total cost of failure multiplied by P_f , cost of construction and total expected cost). The optimal expected total cost that meets the optimal reliability index (RI) can be calculated for each scenario of theses nine scenarios (according to the most two critical parameters). Results showed that the optimal scenario was \$108.85 for the 5th scenario in this study.

4. RESULTS

The results can be classified according to the work accomplished into two categories; the 1st category dealt with FRI model [18] that includes (slope, aspect, curvature and precipitation), against pixels, pixel percent, rockslide occurrence points,

rockslide occurrence points percent, frequency ratio and rock hazard index. The 2nd category dealt with results of the used scenarios which are indicated in a group of charts that represents relationships between costs of construction, cost of failure multiplied by (P_f), the total cost versus (P_f). For obtaining the optimal total expected cost, a comparison between the different optimal values of the scenarios had been accomplished for achieving global optimal for all scenarios.

4.1 Application of Frequency Ratio Index (FRI) Model

Using (FRI) [16], the spatial relationships between rockslide occurrence points and factors contributing to rockslide occurrence (e.g., slope, aspect, curvature and precipitation) were derived and shown in Fig. 3. In Gebel Mokattam area, where most of the catastrophic rockslides occur, the main cause seems to be; a) the presence of active normal faults [19], which greatly appeared after the earthquake of October 1992. b) Limestone blocks full of caves and karst holes due to effect of rains and sewage water leaked deeply from many houses built at the top of the fractured limestone plateau and lie over soft shale beds that likely to slide. c) Using explosions in limestone quarries above the plateau increase its fractures.

The rockslide occurrence points were measured and recorded for each factor's class. The frequency ratio is calculated from analysis of the relationship between rockslides and the attribute factors by counting the pixels in each factor's class then the percentages of this number related to the total number of pixels in the factor (Table 5). Therefore, the frequency ratios of each factor's type were calculated from their relationship with rockslide occurrence points. In relationship analysis, ratio is that of area where rockslides occurred to total area, so that a value of one is an average value.

The greater the frequency ratio value, the higher the hazard to rockslide occurrence and vice versa (Table 5). Accordingly, in Gebel Mokattam area, the slope (degree) has very high RHI (95.31), followed by the aspect direction with high RHI (7.74), then the curvature types with moderate RHI (5.46) and the precipitation (mm) has low RHI (3.75), Table 5 and Fig. 6.

COST BENEFIT ANALYSIS FOR ROCK-SIDE SLOPE FAILURE....

Table 5. Frequency ratio and rock hazard index were calculated for the rockslide-related factors (slope, aspect, curvature and precipitation) in Gebel Mokattam area.

Factor	Class	Pixels in class	Pixel (% ^a)	Rockslide occurrence points	Rockslide occurrence points, (% ^b)	Frequency ratio (^{b/a})	Rock hazard index (RHI)
Slope	0-15°	338,459	92.5	7	20.6	0.22	95.31
	15-25°	17,190	4.7	11	32.35	6.88	
	25-35°	3,739	1.2	12	35.3	29.41	
	35-59°	702	0.2	4	11.76	58.8	
Aspect	Flat	22,611	6.4	0	0	0	7.74
	North	24,243	6.9	2	5.88	0.85	
	Northeast	40,009	11.3	2	5.88	0.52	
	East	32,908	9.3	2	5.88	0.63	
	Southeast	30,714	8.7	0	0	0	
	South	43,114	12.2	7	20.6	1.68	
	Southwest	51,919	14.7	4	11.76	0.8	
	West	54,079	15.28	10	29.4	1.92	
Curvature	Concave	62,853	17.2	10	29.4	1.7	5.46
	Flat	263,560	72	12	35.3	0.5	
	Convex	39,591	10.8	12	35.3	3.26	
Precipitation , mm	1.86-1.90	22,814	6.24	0	0	0	3.75
	1.90-1.93	34,733	9.5	0	0	0	
	1.93-1.95	145,360	39.74	4	11.76	0.3	
	1.95-1.97	93,349	25.52	30	88.23	3.45	
	1.97-2.00	69,460	19	0	0	0	

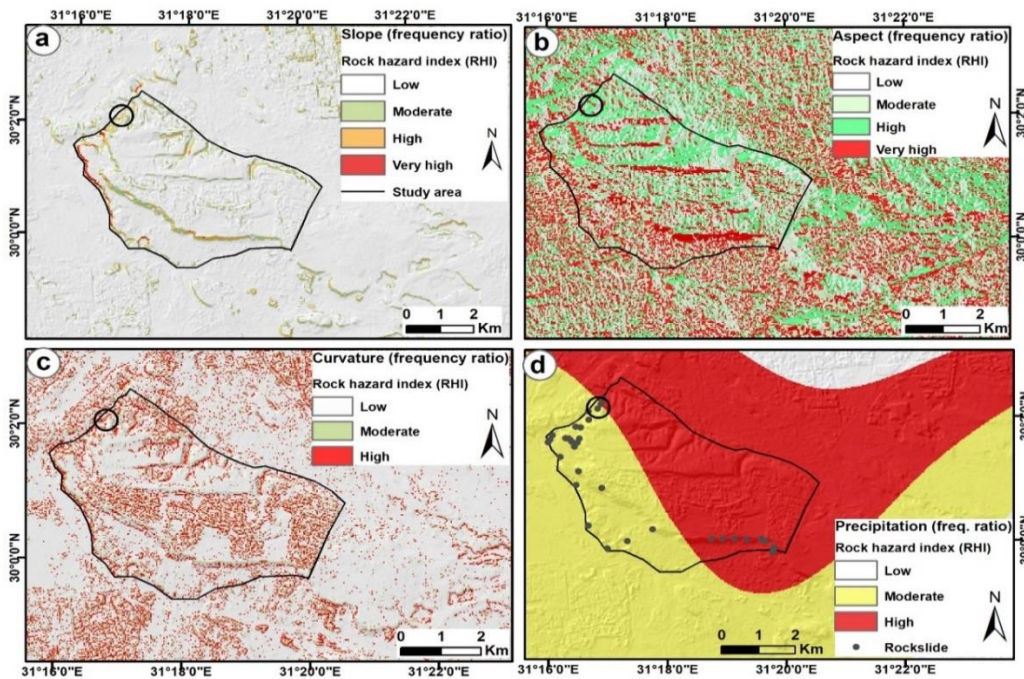


Fig. 6. a) Slope (in degrees) derived from ALOS DEM b) Aspect direction c) Curvature types d) Daily precipitation data.

4.2 The Optimal Cost Value

The results of the scenarios are indicated in a group of charts that represents the relationships between the costs of construction, the cost of failure multiplied by (P_f), the total cost vs (P_f) for obtaining the optimal cost that meets the optimal R.I.

4.2.1 Best scenarios for optimal probability of failure vs optimal total cost

For the curve of the total cost, the larger increase of (P_f) the lower decrease in the total cost value until it reaches the optimal value after that the larger increase of (P_f) the larger increase in the total cost value. It can be seen that the optimal cost values are \$117.23 for 1st scenario, \$112.03 for 2nd scenario, \$113.19 for 3rd scenario, \$115.46 for 4th scenario, \$129.95 for 6th scenario, \$122.07 for 7th scenario, \$118.22 for 8th scenario, and \$121.21 for 9th scenario. The best scenario was \$108.85 for 5th scenario, Fig. 7.

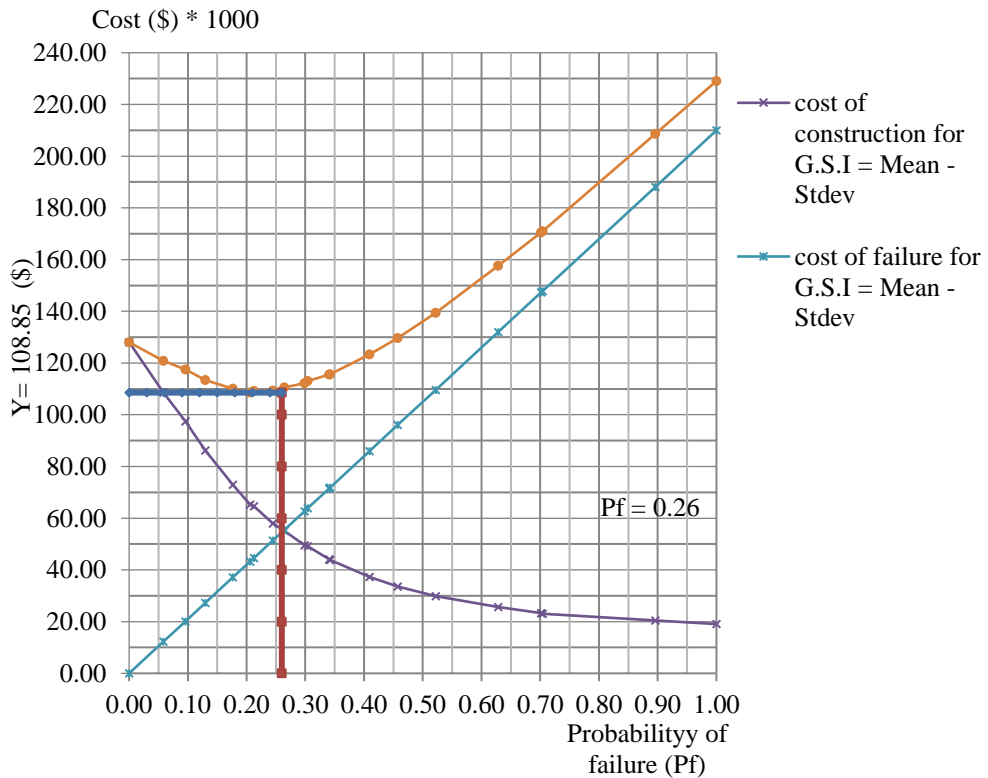


Fig. 7. Relationship between cost of construction cost of failure multiplied by (P_f), total expected cost and (P_f) for upper plateau for the scenario G.S.I = (Mean – SD).

5. CONCLUSIONS

This paper investigated the financial benefits of rockslide prevention measures at Gebel Mokattam area, where the catastrophic rock failure accident occurred in (06/09/2008) in Duwaiqa area, Cairo, Egypt. FRI [18] is created based on the rockslide-related geological and climate factors (e.g. slope, aspect, curvature and precipitation) to highlight the main rockslide conditioning features and the most hazardous and weak points in Mokattam area. Slope was the most hazardous rockslide factor controlling the rock failure in the study area. Numerical modeling showed that corrective works accomplished after the rock failure supporting rock slope such as rock bolts, could improve rock slope stability. A cost benefit analysis was defined that prevention was financially convenient compared to a non-preventive and passive approach.

The focus of this paper is determining the most critical parameters that were normally distributed to reach cost optimization based on the Central Limit Theorem [23], all the studied parameters such as (UCS, Unit Weight and Hoek-Brown's parameters) with samples sizes greater than 30 are normally distributed with minimum effect on the results. The methodology used in this paper is suitable for the rock side slope stability. Hoek Brown Criterion had been used along with the statistical methods, gives simple and easy technique for obtaining optimal total expected cost value that meets the optimal (P_f). The most critical parameters were shortlisted into two main parameters; (UCS) and (GSI) and applied in this paper. Considering such critical parameters, in addition to analyzing their different scenarios; leading to reach the optimal total cost of the slope stability that meets the optimal RI.

Also, this paper deals with the application of the algorithm for obtaining the equations of the expected total cost, cost of construction and cost of failure multiplied by (P_f) for each scenario of the 9 scenarios modeled for UCS and GSI. These different scenarios include a combination values of (mean + SD) for the most two critical parameters (UCS and GSI) to insure obtaining optimal scenario for the optimal RI that meets the optimal expected total cost. The case study of the Upper Plateau of Gebel

Mokattam area indicated that optimal expected cost value occurs at the 5th scenario where GSI = (Mean - SD) with an optimal total expected cost value of \$108.85.

DECLARATION OF CONFLICT OF INTERESTS

The authors have declared no conflict of interests.

REFERENCES

1. Soliman, A., Bekhit, H., Hamed, K., and El Zawahry, A., "Prediction of Dam Breach Parameters and their Uncertainties", *Journal of Engineering and Applied Science*, Vol. 61, No. 3, pp. 269-290, 2014.
2. Cai, M., Kaiser, P., Uno, H., Tasaka, Y., and Minami, M., "Estimation of Rock Mass Deformation Modulus and Strength of Jointed Hard Rock Masses using the GSI System", *International Journal of Rock Mechanics and Mining Sciences*, Vol. 41, pp. 3-19, 2004.
3. Deng, D., Li, L., and Zhao, L., "Limit Equilibrium Method (LEM) of Slope Stability and Calculation of Comprehensive Factor of Safety with Double Strength-Reduction Technique", *Journal of Mountain Science*, Vol. 14, pp. 2311-2324, 2017.
4. Merifield, R. S., Lyamin, A. V., and Sloan, S. W., "Limit Analysis Solutions for the Bearing Capacity of Rock Masses using the Generalised Hoek-Brown Criterion", *International Journal of Rock Mechanics and Mining Sciences*, Vol. 43, No. 6, pp. 920-937, 2006.
5. Li, S., Liu, Y., He, X., and Liu, Y., "Global Search Algorithm of Minimum Safety Factor for Slope Stability Analysis Based on Annealing Simulation", *Chinese Journal of Rock Mechanics and Engineering*, Vol. 22, No. 2, pp. 236-240, 2003.
6. Potgieter, J. T., "Finite Element Versus Limit Equilibrium Stability Analyses for Surface Excavations", M. Eng. Thesis, University of Pretoria, 2016.
7. Wang, Y., Cao, Z., and Li, D., "Bayesian Perspective on Geotechnical Variability and Site Characterization", *Engineering Geology*, Vol. 203, pp. 117-125, 2015.
8. Guzzetti, F., "Forecasting Natural Hazards, Performance of Scientists, Ethics, and the Need for Transparency", *Toxicological and Environmental Chemistry*, Vol. 98, No. 9, pp. 1043-1059, 2015.
9. Corominas, J., Van Westen, C., Frattini, P., Cascini, L., Malet, J.-P., Fotopoulou, S., and Smith, J. T., "Recommendations for the Quantitative Analysis of Landslide Risk", *Bulletin of Engineering Geology and the Environment*, Vol. 73, No. 2, pp. 209-263, 2013.
10. Hilker, N., Badoux, A., and Hegg, C., "The Swiss Flood and Landslide Damage Database 1972-2007", *Natural Hazards and Earth System Sciences*, Vol. 9, No. 3, pp. 913-925, 2009.

11. Salbego, G., Mario, F., Enrico, B., Toaldo, M., and Rinaldo, G., “Detailed and Large-Scale Cost/Benefit Analyses of Landslide Prevention vs. Post-Event Actions”, *Natural Hazards and Earth System Science*, Vol. 15, pp. 2461-2472, 2015.
12. Guzzetti, F., and Tonelli, G., “Information System on Hydrological and Geomorphological Catastrophes in Italy: A Tool for Managing Landslide and Flood Hazards”, *Natural Hazards and Earth System Sciences*, Vol. 4, No. 2, pp. 213-232, 2004.
13. Guettiche, A., Guéguen, P., and Mimoune, M., “Economic and Human Loss Empirical Models for Earthquakes in the Mediterranean Region, with Particular Focus on Algeria”, *International Journal of Disaster Risk Science*, Vol. 8, No. 4, pp. 415-434, 2017.
14. Crozier, M. J., and Thomas, G., “Landslide Hazard and Risk: Issues, Concepts and Approach”, *Landslide Hazard and Risk*, John Wiley and Sons Ltd., 2005.
15. Pellicani, R., Westen, C. J., and Giuseppe, S., “Assessing Landslide Exposure in Areas with Limited Landslide Information”, *Landslides*, Vol. 11, pp. 463-480, 2014.
16. Boonyanuphap, J., “Cost-Benefit Analysis of Vetiver System-Based Rehabilitation Measures for Landslide-Damaged Mountainous Agricultural Lands in the Lower Northern Thailand”, *Natural Hazards*, Vol. 69, No. 1, pp. 599-629, 2013.
17. ESRI, “ArcGIS Desktop: Release 10”, Redlands, 2011.
18. Pradhan, B., and Lee, S., “Delineation of Landslide Hazard Areas using Frequency Ratio, Logistic Regression and Artificial Neural Network Model at Penang Island, Malaysia”, *Environmental Earth Sciences*, Vol. 60, No. 5, pp. 1037-1054, 2009.
19. Poscolieri, M., Parcharidis, I., Fomelis, M., and Rafanelli, C., “Ground Deformation Monitoring in the Greater Cairo Metropolitan Region (Egypt) by SAR Interferometry”, *Environmental Semeiotics*, Vol. 4, No. 3, pp. 17-45, 2011.
20. Mohamed, S. A., “Engineering Geology of Some Areas in the Greater Cairo”, Ph. D. Thesis, Ain Shams University, 1985.
21. Thompson, A. G., and Villaescusa, E., “Case Studies of Rock Reinforcement Components and Systems Testing”, *Rock Mechanics and Rock Engineering*, Vol. 47, pp. 1589-1602, 2014.
22. <https://www.fhwa.dot.gov/engineering/geotech/pubs/nhi14007.pdf>, (Accessed 20/12/2020).
23. Kwak, S.G., and Jong Hae Kim, J.H., “Central Limit Theorem: The Cornerstone of Modern Statistics”, *Korean Journal of Anesthesiology*, Vol. 70, No. 2, pp. 144, 2017.
24. Huffman, G. J., Bolvin, D. T., Braithwaite, D., Hsu, K., Joyce, R., Kidd, C., Nelkin, E. J., Sorooshian, S., Tan, T., and Xie, P., “Algorithm Theoretical Basis Document (ATBD) Version 5.2 NASA”, *NASA Global Precipitation Measurement (GPM) Integrated Multi-satellitE Retrievals for GPM (IMERG)*, Basis Doc. IMERG Algo, pp. 1-31, 2018.

تحليل فائدة التكلفة لمنع إنهيار الميول الصخرية الجانبية باستخدام التصميم القائم على الموثوقية

يحلل هذا البحث الفائدة الاقتصادية لإجراءات الوقاية من الإنهيارات الصخرية في منطقة جبل المقطم، بالقاهرة، حيث وقع حادث انهيار صخري في ٦/٩/٢٠٠٨م. هذا وقد تم تطبيق مؤشر نسبة التردد (FRI)، المبني على العوامل الجيولوجية والمناخية المرتبطة بالانزلاق الصخري، والذي يسلط الضوء على الخصائص الرئيسية للانزلاق الصخري والقطاعات الأكثر خطورة بمنطقة المقطم. ويمثل مؤشر نسبة التردد (FRI)، وهو النسبة بين احتمالات حدوث الانزلاق الصخري إلى احتمالات عدم حدوثه داخل كل مجموعة لكل معامل من المعاملات الجيولوجية والمناخية. وأظهرت النتائج أن معامل إنحدار الجوانب الصخرية هو أكثر المعاملات خطورة. لذلك تم دعم الميول الصخرية باستخدام المسامير الصخرية. وذلك بعد الحصول على أكثر أماكن الخطر المعرضة للانهدام الصخري، ثم يتم حساب التكلفة الإجمالية المثلى التي تلبي مؤشر الموثوقية الأمثل. حيث أنه قد تم إختصار هذه المعاملات في عاملين رئيسيين هما قوة الانضغاط أحادي المحور (UCS) ومؤشر القوة الجيولوجية (GSI)، وبتحليل التسع سيناريوهات المختلفة لهذين المعاملين؛ فإن هذا يؤدي إلى الوصول إلى التكلفة الإجمالية المثلى لاستقرار المنحدر التي تلبي مؤشر الموثوقية الأمثل.